Title

Nitrous oxide emissions from inland waters: Are IPCC estimates too high?

Journal

Global Change Biology, 25(2)

ISSN

1354-1013

Authors

Maavara, Taylor

Lauerwald, Ronny

Laruelle, Goulven G

et al.

Publication Date

2019-02-01

DOI

10.1111/gcb.14504

Peer reviewed

Nitrous oxide emissions from inland waters: Are IPCC estimates too high?

Taylor Maavara[1,2] | Ronny Lauerwald[2,3] | Goulven G. Laruelle[2,4,5] | Zahra Akbarzadeh[6] | Nicholas J. Bouskill[1] | Philippe Van Cappellen[6] | Pierre Regnier[2]

[1] Earth and Environmental Sciences Area, Lawrence Berkeley National Laboratory, Berkeley, California [2] Department Geoscience, Environment & Society, Université Libre de Bruxelles, Brussels, Belgium [3] Department of Mathematics, College of Engineering, Mathematics and Physical Sciences, University of Exeter, Exeter, UK [4] UMR 7619 Metis, Sorbonne Universités, UPMC, Univ Paris 06, CNRS, EPHE, IPSL, Paris, France [5] FR636 IPSL, Sorbonne Universités, UPMC, Univ Paris 06, CNRS, Paris, France [6] Ecohydrology Research Group, Water Institute, Department of Earth and Environmental Sciences, University of Waterloo, Waterloo, Ontario, Canada

Correspondence Taylor Maavara, Earth and Environmental Sciences Area, Lawrence Berkeley National Laboratory, Berkeley, CA. Email: tmaavara@lbl.gov

Abstract

Nitrous oxide (N_2O) emissions from inland waters remain a major source of uncertainty in global greenhouse gas budgets. N_2O emissions are typically estimated using emission factors (EFs), defined as the proportion of the terrestrial nitrogen (N) load to a water body that is emitted as N_2O to the atmosphere. The Intergovernmental Panel on Climate Change (IPCC) has proposed EFs of 0.25% and 0.75%, though studies have suggested that both these values are either too high or too low. In this work, we develop a mechanistic modeling approach to explicitly predict N_2O production and emissions via nitrification and denitrification in rivers, reservoirs and estuaries. In particular, we introduce a water residence time dependence, which kinetically limits the extent of denitrification and nitrification in water bodies. We revise existing spatially explicit estimates of N loads to inland waters to predict both lumped watershed and half-degree grid cell emissions and EFs worldwide, as well as the proportions of these emissions that originate from denitrification and nitrification. We estimate global inland water N_2O emissions of 10.6–19.8 Gmol N year^{-1} (148–277 Gg N year^{-1}), with reservoirs producing most N_2O per unit area. Our results indicate that IPCC EFs are likely overestimated by up to an order of magnitude, and that achieving the magnitude of the IPCC's EFs is kinetically improbable in most river systems. Denitrification represents the major pathway of N_2O production in river systems, whereas nitrification dominates production in reservoirs and estuaries.

1 INTRODUCTION

Nitrous oxide (N_2O) is an ozone-depleting greenhouse gas (GHG), considered to be the third most important GHG contributing to radiative forcing and

global climate change (Neubauer & Megonigal, 2015; Ravishankara, Daniel, & Portmann, 2009; Syakila & Kroeze, 2011). Most N_2O is produced by microbial processes such as nitrification and denitrification in terrestrial and aquatic systems, including rivers, estuaries, coastal seas and the open ocean (Freing, Wallace, & Bange, 2012). The production of N_2O shows large spatial and temporal variability and emission estimates for aquatic systems are uncertain. In particular, emissions from rivers, estuaries and continental shelves have been the subject of debate for many years (De Klein et al., 2006; Seitzinger & Kroeze, 1998). The 5th IPCC Assessment Report (Ciais et al., 2013) proposed that, together, rivers, estuaries and coastal zones emit 0.6 Tg N (N_2O) $year^{-1}$ (based on IPCC's 2006 guidelines, Kroeze, Dumont, & Seitzinger, 2010; Syakila & Kroeze, 2011). This corresponds to about 3% of all N_2O emissions and about one third of IPCC's previous estimate of 1.7 Tg N $year^{-1}$ in the 4th Assessment Report for the same systems. Several studies have highlighted that emissions from rivers might be underestimated (Beaulieu et al., 2011) or significantly overestimated (Hu, Chen, & Dahlgren, 2016; Macdonald, Nadelko, Chang, Glover, & Warneke, 2016) in the IPCC assessments (Table 1). A recent review of estuarine emissions (Murray, Erler, & Eyre, 2015) also suggested that these aquatic systems could emit about three times more N_2O (0.31 Tg N $year^{-1}$) than the latest IPCC estimate. Recently, Deemer et al. (2016) provided the first global estimate of N_2O evasion from dam reservoirs at 0.03 Tg N $year^{-1}$.

TABLE 1 Literature survey of all published global estimates for N_2O emissions for rivers, reservoirs and estuaries. The table provides the source of the N loads used for the calculations, its value (and under which form, that is, Total N—TN, Total Dissolved N—TDN, or Dissolved Inorganic N—DIN), the N_2O emission factor, the global N_2O emissions and an estimate of the corresponding emission rate per surface area. The latter are calculated using published estimates of the surface areas of rivers (Downing et al., 2012), reservoirs (Lehner et al., 2011) and estuaries (Dürr et al., 2011)

Study	N loads	N load value (10^3 Gg N $year^{-1}$)	Emission factor (%)	Global N_2O emission (Gg N $year^{-1}$)	N_2O emission rate (g N m^{-2} $year^{-1}$)
Rivers (662×10^3 km^2)					
Seitzinger and Kroeze (1998) and Seitzinger et al. (2000)[a]	NEWS model	41.6 DIN	2.5	1,050 (190–1870)	1.59 (0.29–2.82)
Kroeze et al. (2005)[a]	NEWS model	50.3 DIN	2.5	1,256	1.90
Mosier et al. (1998)[b]	IPCC	93 TN	0.75	700	1.06
De Klein et al. (2006)[c]	IPCC	93 TN	0.25	350	0.53
Kroeze et al. (2010)[d]	NEWS model	88 TN 60 TDN	0.25 or 2.5	300–2,100	0.45–3.17
Beaulieu et al. (2011)[e]	IPCC	90 TN	0.75	680	1.03
Hu et al. (2016)[f]	NEWS	18.8 DIN	0.17 (0.08–0.31)	32.2 (12.4–66.9)	0.05 (0.02–0.10)
This study	Derived from NEWS	184.3 TN	Scenario dependent	45.6–49.4	0.07
Reservoirs (45×10^3 km^2)					
Deemer et al. (2016)[g]	Bottom-up (n = 58)	NA	NA	30 (20–70)	0.67 (0.44–1.56)
This study	Derived from NEWS	61 TN	Scenario dependent	42.4–71.5	0.94–1.6
Estuaries ($1{,}067 \times 10^3$ km^2)					
Law et al. (1992)	Bottom-up (n = 5)	NA	NA	220	0.20
Bange, Rapsomanikis, and Andreae (1996)	Bottom-up (n = 12)	NA	NA	3,700–5,700	3.47–5.34
Robinson et al. (1998)	Bottom-up (n = 4)	NA	NA	130–450	0.12–0.42
Seitzinger and Kroeze (1998)	NEWS model	20.8 DIN	1	220 (70–690)	0.21(0.06–0.65)
De Wilde and De Bie (2000)	Bottom-up (n = 1)	NA	NA	1,500	1.41
Kroeze et al. (2005)	NEWS model	25 DIN	1	250	0.24
Kroeze et al. (2010)[h]	NEWS Model	44 TN 30 TDN	0.25 or 2.5	100–600	0.09–0.56
Murray et al. (2015)[i]	Bottom-up (n = 56)	NA	NA	310 (150–910)	0.29 (0.14–0.85)
This study	Derived from NEWS	97.5 TN	Scenario dependent	60.0–155.4	0.06–0.15

[a]Based on four studies with 0.3% and 3% (N_2O:N_2) for DIN load of <10 and >10 kg N ha^{-1} $year^{-1}$, respectively. [b]Based on six studies made in Europe and North America. [c]Based on two studies in England and New Zealand for relatively short river systems. [d]IPCC default EF5-r (0.25%) was used for low case and 2.5% was assumed as the high case based onSeitzinger and Kroeze (1998). [e]Based on observations conducted for 72 headwater streams in North America with 0.25% observed for denitrification and 0.5% assumed for nitrification. [f]Based on meta-analysis of global data with 169 observations covering a wide range of rivers. [g]Based on mean flux density from 58 measurements, multiplied by reservoir surface area (GranD, Lehner et al., 2011). [h]IPCC default EF5-r (0.25%) was used for low case and 2.5% was assumed as the high case based onSeitzinger and Kroeze (1998). [i]Based on mean flux density from 56 measurements, multiplied by estuarine and tidal surface areas (average of Dürr et al., 2011; Woodwell, Rich, & Hall, 1973).

Global N_2O flux estimations from open inland waters (rivers, reservoirs and estuaries) have followed two distinct approaches. The first approach involves upscaling direct N_2O flux measurements from aquatic systems, by multiplying local fluxes by the estimated global areal extents of water bodies. This methodology has been followed by Deemer et al. (2016) for reservoirs and by Bange (2006), Law, Rees, and Owens (1992), Robinson, Nedwell, Harrison, and Ogilvie (1998), de Wilde and de Bie (2000) and Murray et al. (2015) for estuaries. To our knowledge, this approach has never been applied to estimate river N_2O emissions globally. The most recent global N_2O budgets rely on 58 local measurements in reservoirs (Deemer et al., 2016) and 74 local measurements in estuarine environments (Murray et al., 2015) including open waters, mangroves, intertidal sediments, salt marshes and seagrasses. According to Murray et al. (2015), about 75% of the estuarine N_2O evasion originates from open water bodies, that is, the portion

of estuaries flooded throughout the entire tidal cycle. In addition to the uncertainties associated with using a limited pool of data to generate global estimates, uncertainties arise from the highly skewed spatial distributions of the local datasets, which are focused in industrialized countries, and from the uncertainties associated with the estimated areal extents of different types of water bodies (Dürr et al., 2011; Laruelle et al., 2013; Lehner et al., 2011).

The second approach for estimating large-scale N_2O emissions relies on semi-empirical models, in which N_2O emission rates are calculated as the product of an emission factor (EF) and estimates of N loading to water bodies. However, both N load estimates and EFs are subject to large uncertainties. In particular, EFs (generally defined as the fraction of N load to the water body that is emitted as N_2O–N) vary by more than one order of magnitude, with reported values ranging from 0.17% to 5.6% (Beaulieu et al., 2011; Hu et al., 2016; Seitzinger & Kroeze, 1998). Several studies argue that the current default IPCC EF used to estimate worldwide emissions (0.25%) may be either overestimated (Clough, Buckthought, Casciotti, Kelliher, & Jones, 2011; Clough, Buckthought, Kelliher, & Sherlock, 2007; Kroeze et al., 2010) or underestimated (Beaulieu et al., 2011; Yu et al., 2013). Much of the disagreement arises from local values differing substantially from IPCC's default EF values, due to factors such as intense urbanization (where there may be disproportionately high emissions, e.g., Yu et al., 2013) or diurnal variability (where in-stream concentrations decrease at night, indicating that the majority of studies that sample during the day may overestimate emissions e.g., Clough et al., 2007). Kroeze et al. (2010) further discuss the uncertainty associated with whether the EF is taken with regard to total N (TN) or dissolved inorganic *N* (DIN) loads to the water body (Table 1), as TN includes refractory N species while DIN excludes other bioavailable species. Inconsistencies in assumptions and methodologies such as these confound our ability to make direct comparisons between literature estimations.

Model-derived estimates of global N_2O evasion ruire inclusion of natural as well as anthropogenic N loadings, of which the anthropogenic loadings are dominant in most river systems (Seitzinger, Kroeze, & Styles, 2000). For rivers, loadings have been constrained using the IPCC methodology (Mosier et al., 1998), which assumes that the only TN sources are from global synthetic fertilizer use and N excreted by livestock, with 30% lost to leaching and surface runoff. The Global Nutrients in Watersheds (NEWS) model (Dumont, Harrison, Kroeze, Bakker, & Seitzinger, 2005; Mayorga et al., 2010) computes DIN and TN loadings according to empirical relationships between loading and an array of controlling factors including biophysical watershed characteristics, population density, socioeconomics, land cover and land use and climatic conditions. Discrepancies in N_2O evasion between studies can partly be explained by different N load estimates (Table 1). For estuaries, only the NEWS model approach has been used, with the inputs derived from

the NEWS loads delivered to coastal zones (Seitzinger & Kroeze, 1998; Seitzinger, Harrison, Dumont, Beusen, & Bouwman, 2005).

All model studies scale the global N_2O emissions to the N loads, either considering only DIN (Beaulieu et al., 2011; Hu et al., 2016; Seitzinger & Kroeze, 1998), or including dissolved inorganic, organic and particulate N forms (DIN +DON + PN =TN) together (Mosier et al., 1998; Syakila & Kroeze, 2011). This upscaling can either be done directly by applying an EF to the N load following the IPCC methodology of Mosier et al. (1998), or via an intermediate step (Seitzinger & Kroeze, 1998) where N loads are first used to constrain global denitrification and nitrification rates and, next, N_2O emissions are assumed to be fixed fractions of these N transformation pathways. Nevertheless, the second approach is somewhat equivalent to the first because all studies have so far assumed that the N lost via denitrification and the N oxidized via nitrification are themselves fixed fractions of TN or DIN loadings (Beaulieu et al., 2011; Seitzinger & Kroeze, 1998).

By far, most of the differences in model-derived estimates result from the choice of prescribed fractions of N loads which are lost in the form of N_2O, either via the direct approach or via the intermediate step of estimated denitrification-nitrification rates. With the notable exception of the recent study by Hu et al. (2016), all studies have applied EFs and fractions determined from a very limited number of observations, and their values have thus been subject to intense debate in past decades. Interestingly, the proposed EF of Hu et al. (2016), based on a meta-analysis of 169 N_2O flux observations covering a wide range of rivers, is significantly lower (0.17%) than previously applied values. Similarly, the fraction of N that is oxidized via nitrification has been traditionally scaled to denitrification rates, but the scaling factor has varied between 1 and 2 among various studies (Kroeze, Dumont, & Seitzinger, 2005; Seitzinger & Kroeze, 1998; Seitzinger et al., 2000).

All models applied thus far have relied on simple semi-empirical approaches. As pointed out by Ivens, Tysmans, Kroeze, Löhr, and Wijnen (2011), alternative approaches that better account for spatial variability and model uncertainties should be developed. More specifically, developing a global-scale mechanistic model that represents both N cycling and transport rates in a spatially and dynamically explicit way remains a critical priority. Such a mechanistic model should include representations of nitrification, denitrification and N assimilation rates, as well as N_2O inputs from land and N_2O production and transport along the river system (Ivens et al., 2011). This objective is particularly timely because Beaulieu et al. (2011) have recently reported denitrification N_2O yields (percentage of denitrified N released as N_2O) for a number of streams and rivers (n = 72) that can be used to parameterize a mechanistic modeling approach.

In a first step in this direction, we have developed the first integrated model of global N_2O emissions along the entire land-ocean aquatic continuum (LOAC). We focus our study on open waters, including rivers, dammed reservoirs and estuaries. This analysis does not include lakes or wetlands including freshwater wetlands, seagrasses, salt marshes, intertidal sediments, mangroves, or coastal aquaculture ponds. We calculate DIN, DON and PN yields in watersheds worldwide, and track the changes to these species' loads as they are delivered to rivers, reservoirs and estuaries. We quantify cascading TN losses via burial and denitrification, and additions via N fixation. In each water body, we quantify the N_2O emissions associated with in-stream, in-estuarine or in-reservoir denitrification and nitrification. We contextualize the results of our model by performing a scenario-based uncertainty analysis, which relies on the range of emissions factors reported in the existing literature. We further compare to existing global estimates for both anthropogenic and natural N_2O emissions. Through our explicit quantification of the interacting changes of N loads along the LOAC and of the load-specific N_2O production mechanisms, our study represents the most comprehensive estimate of LOAC N_2O emissions to date.

2 MATERIALS AND METHODS

2.1 Overview

A mechanistic mass balance model was developed to represent generalized stream, reservoir and estuarine N fluxes and transformations (Figure 1). The model development followed an approach similar to that used for phosphorus (P) (Maavara et al., 2015), organic carbon (OC) (Maavara, Lauerwald, Regnier, & Van Cappellen, 2017) and *N* (Akbarzadeh, Maavara, Slowinski, & Van Cappellen) cycling in dam reservoirs. River, reservoir and estuary kinetic parameters associated with physical and biogeochemical processes were implemented using probability density functions (PDFs) that account for the global distributions of the corresponding parameter values. The fluxes in the model represent lumped sediment-water column rates and were resolved at the annual timescale. Water residence time controls the magnitude of the in-system transformation and elimination fluxes through an inverse relationship with nutrient effluxes from the water body. The N_2O model was coupled to OC and P models of (Maavara et al., 2017, 2015) in order to represent P- and OC-dependencies into processes such a primary productivity and N fixation.

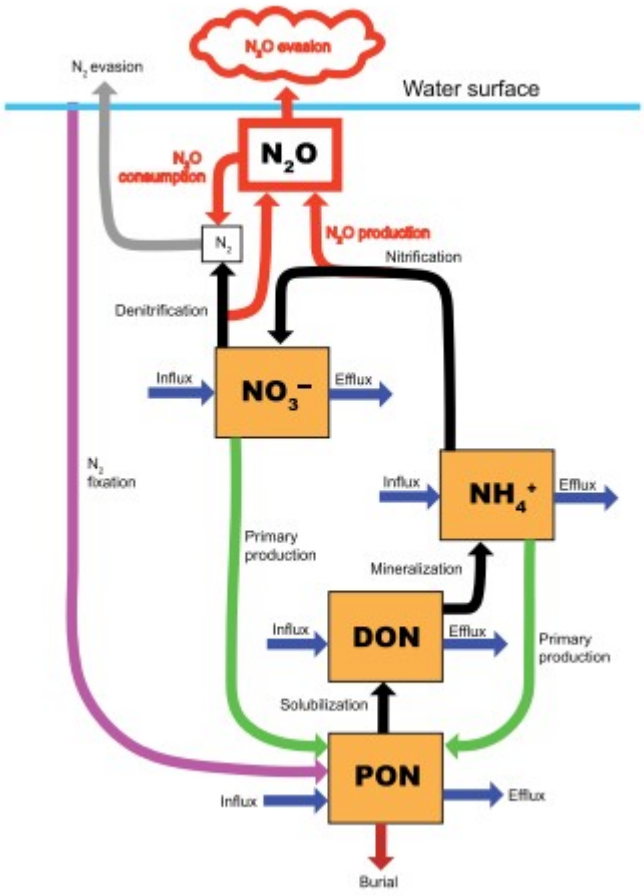

Figure 1. Mechanistic box model used to represent reservoir, river and estuarine nitrogen dynamics. Note that N_2 concentrations and evasion are shown for completeness, but not explicitly represented in the model

A Monte Carlo analysis of the model was performed, in which parameters were randomly selected from the pre-assigned PDFs. After 6,000 iterations, a database of hypothetical worldwide N dynamics, including N_2O production and emissions, was generated for inland open waters. Each of the 6,000 Monte Carlo realizations combined a unique set of parameter values obtained stochastically from the PDFs to quantify rates and fluxes for all N cycling processes. Next, global relationships relating N processes and N_2O emissions to water residence time and TN loads were extracted from the Monte Carlo output. These relationships were then applied to N loads delivered to all river, reservoir and estuarine systems along a spatially routed network representing the global LOAC. We predicted N loads following the methods used in the NEWS model and described in Mayorga et al. (2010). Rather than applying an average EF to all water bodies, the use of water residence time as independent variable explicitly adjusts for the extent of N_2O production and emission that is kinetically possible within the timeframe available in a given water body. In the following sections, we describe the modeling steps and parameter constraints in detail.

2.2 Emission factors: terminology

Emission factors (EFs) have variable definitions throughout the literature. In this study, we utilize a variety of these literature definitions in addition to our own to develop a suite of scenarios based on a variety of assumptions related to N_2O emissions. Henceforth, the following EF definitions apply:

$$EF(a)_{denit} = \frac{N_2O_{em}}{Denit} \quad (1)$$

$$EF(a)_{nitrif} = \frac{N_2O_{em}}{Nitrif} \quad (2)$$

$$EF(b)_{denit} = \frac{N_2O_{prod,net}}{Denit} \quad (3)$$

$$EF(c)_{denit} = \frac{N_2O_{prod}}{Denit} \quad (4)$$

$$EF(c)_{nitrif} = \frac{N_2O_{prod}}{Nitrif} \quad (5)$$

and

$$EF(d)_{nitrif} = \frac{N_2O_{em}}{TN_{in}} \quad (6)$$

where N_2O_{em} is the annual flux of N_2O emitted across the water-air interface relative to the nitrification or denitrification flux, Denit is the annual denitrification flux, Nitrif is the annual nitrification flux, N_2O_{prod} is the annual production of N_2O in the water body via nitrification or denitrification, $N_2O_{prod,net}$ is the annual production of N_2O via denitrification minus the N_2O subsequently transformed to N_2, and TN_{in} is the annual riverine load of total N delivered to the water body. In the literature, EF(*d*) has typically been used as the conventional definition.

2.3 Mechanistic modeling approach

The N pools in the model were nitrate (NO_3^-) and ammonium (NH_4^+), dissolved organic *N* (DON) and particulate organic *N* (PON) pools, and the key transformation and transport fluxes associated with these species (Figure 1). Specifically, we took into account the influxes and effluxes of NH_4^+, NO_3^-, DON and PON to and from water bodies, primary productivity, PON solubilization and burial, mineralization of DON, nitrification, denitrification, plus N_2O production and consumption via the latter two processes, and N_2O exchanges with the atmosphere. Each model realization was solved using the Runge–Kutta 4 integration method, with a 0.01-year time step and, in the case of reservoirs, run for the number of years since dam closure, or for at least 100 years in the case of rivers and estuaries, hence ensuring steady state conditions were reached under the majority of parameter combinations in the Monte Carlo simulations. We constrained one

PDF for rivers, reservoirs and estuaries as a compiled dataset. In this section, we will focus on describing the model parameters specifically associated with N_2O production and emissions. A full description of the parameterization of the physical and other biogeochemical processes included in the model can be found in Section S1.

Two approaches were used to bracket our estimates of N_2O emissions from inland waters. For both model structures, N_2O production in mol N year^{-1} was obtained from:

$$N_2O_{prod} = EF(b)_{denit} \times Denit + EF(c)_{nitrif} \times Nitrif \quad (7)$$

In the first, more simple, approach (referred to as Default Scenario 1, or DS1), N_2O emissions were calculated by multiplying average EF(b)$_{denit}$ and EF(c)$_{nitrif}$ values of 0.9%, proposed by Beaulieu et al. (2011), by model-calculated nitrification and denitrification fluxes (see Section S1), assuming all N_2O_{prod} was emitted to the atmosphere. A Monte Carlo simulation was performed, generating 6,000 hypothetical "observations" from which globally applicable relationships were extracted that relate denitrification, nitrification and N_2O emissions to water residence times and TN loads (TN_{in}, mol year^{-1}). Nitrification in rivers, reservoirs and estuaries was fitted to the following equation:

$$Nitrif = (TN_{in} + Fix)[0.5144 \times erf(0.3692\tau_r)];\ R^2 = 0.16 \quad (8)$$

where Fix is the fixation flux in mol/year, calculated using Equations S6 and S7. Denitrification was similarly fitted to:

$$Denit = (TN_{in} + Fix)[0.3833 \times erf(0.4723\tau_r)];\ R^2 = 0.29 \quad (9)$$

Nitrif and Denit were multiplied by EF(b)$_{denit}$ = EF(c)$_{nitrif}$ = 0.9% for each river, reservoir and estuary worldwide, where we assumed that EF(b)$_{denit}$ = EF(a)$_{denit}$ and EF(c)$_{nitrif}$ = EF(a)$_{nitrif}$.

In the second scenario (Default Scenario 2, or DS2), we explicitly included N_2O as a pool in the model (Figure 1), with Equation (7) representing the input to the N_2O pool. To account for consumption of N_2O produced via denitrification in water bodies with long residence times (τ_r), we computed the inverse of Equation (9) and multiplied it by an average value of EF(c)$_{denit}$ of 0.9% (Figure S6). The resulting emission factor associated with denitrification was therefore:

$$EF(b)_{denit} = EF(c)_{denit} \times 0.4372\, erfc(0.4697\tau_r) \quad (10)$$

For nitrification, EF(c)$_{nitrif}$ was assumed equal to 0.9% with no further scaling because there is no N_2O consumption step associated with nitrification. We then calculated the emissions, N_2O_{em}, assuming that only the fraction of N_2O that is super-saturated with respect to the equilibrium atmospheric N_2O concentration ($[N_2O]_{sat}$) was emitted. In other words:

$$[N_2O]_{sat} = K_H \times pN_2O_{atm} \quad (11)$$

and

$$N_2O_{em} = ([N_2O]_{aq} - [N_2O]_{sat}) \times Q \quad (12)$$

where $[N_2O]_{aq}$ is the concentration of N_2O in the water body calculated by the model, and pN_2O_{atm} is the average atmospheric partial pressure of N_2O, equal to 315 ppb in year 2000 (EPA 2016), and K_H is the temperature dependent Henry's Law coefficient, equal to 2.4×10^{-4} 2006 mol m^{-1} Pa^{-1}at 298.15 K, and temperature corrected to model-predicted temperatures (see Section S1) using the Van't Hoff equation. The gradient between actual and equilibrium concentration is multiplied by the amount of water passing through that system per year Q (km^3/year). Using this emission estimate, it was possible to back-calculate $EF(a)_{denit}$, $EF(a)_{nitrif}$ and EF(d) for comparison with literature values. Equations (11) and (12) assume that, on a yearly time scale, aqueous N_2O reaches equilibrium with the atmosphere (Note: for shorter times scales, more sophisticated kinetics-based approaches may be more appropriate, e.g., Lauerwald et al., 2017).

A second Monte Carlo simulation was run for DS2, and from the output, we fitted a single equation for the total N_2O emissions in rivers, reservoirs and estuaries:

$$N_2O_{em,total} = TN_{in}[a \times erf(b \times \tau_r)] \quad (13)$$

where a = 0.002277 and b = 1.63 (R^2 = 0.11, Figure S1a). Though the literature is divided on whether emissions should be normalized to the TN or DIN load, we chose to normalize our estimates of N_2O emissions and denitrification to TN because this yielded better fits of the entire set of equations to the Monte Carlo data than using DIN. The fraction of the total N_2O produced in the water body originating from denitrification was fitted to a Gaussian function:

$$fraction(N_2O_{prod,denit}) = \left[c \times \exp\left(-\frac{\tau_r - d}{e}\right)^2\right] \quad (14)$$

where c = 0.7789, d = −1.366 and e = 2.751 (R^2 = 0.66, Figure S1b). Equation (13) was multiplied by Equation (14) to obtain the N_2O evasion from denitrification. Evasion from nitrification was then calculated as the difference between total evasion and that associated with denitrification.

2.4 Application to global river network

To calculate the cascading loads of TN delivered to each water body along the river–reservoir–estuary continuum, we spatially routed reservoirs from the Global Reservoirs and Dams (GRanD) database (Lehner et al, 2011), with river networks from Hydrosheds 15s (Lehner, Verdin, & Jarvis, 2008) and Hydro1K (USGS, 2000) at higher latitudes, which was in turn connected to estuaries as represented in the “Worldwide Typology of Nearshore Coastal Systems” of Dürr et al. (2011). A detailed description of the process used to develop this global water body network is given in Section S2 and Figure S2.

To calculate biogeochemical transformation rates and emission fluxes for river reaches, reservoirs and estuaries in a consistent way, the water residence times for each of these water bodies was required. For rivers, the average travel distance (Length, km) along an undammed reach discharging into a reservoir or estuary was estimated using the empirical equation of Rosso, Bacchi, and Barbera (1991):

$$Length = 1.52 \times W_{k,undammed}^{0.58} \quad (15)$$

where $W_{k,\text{undammed}}$ is the undammed catchment area upstream of the kth dam or estuary in km^2. The undammed upstream $W_{k,\text{undammed}}$ is defined for each dam and estuary as the total tributary area from which water flows in without passing another dam. The total upstream areas of all the dams and estuaries were spatially delineated based on the Hydrosheds15s (Lehner et al., 2008) and Hydro1k (USGS, 2000) data sets. They were calculated by subtracting the upstream areas of other dams were overlays occurred. For each dam, the contributing area was derived from the Hydrosheds15s and/or Hydro1k routing schemes. In river catchments with multiple dams, the travel distance of water flowing out of a given dam to the next downstream dam or estuary was calculated as the shortest distance between the dams, or between the dam and the receiving estuary. This distance was multiplied by a sinuosity index of 2.26 (Shen, Anagnostou, Mei, & Hong, 2017) to estimate the actual travel distance. Next, the water residence time along the given river segment was estimated by dividing the travel distance by an average flowing velocity of 0.6 m/s for tributaries and 0.8 m/s for the river main stem (Schulze, Hunger, & Döll, 2005).

For reservoirs, the residence time was calculated using the representative storage capacity (volume) divided by the annual discharge reported in GRanD (Lehner et al., 2011). Only dams constructed during or before year 2000 were included. For estuaries, water residence times were derived from the nearshore coastal systems database compiled by Dürr et al. (2011), which includes estuarine residence times from the literature for 130 systems that account for 20% of the world's TN loads from rivers. Following McKee, Aller, Allison, Bianchi, and Kineke (2004), it was assumed that most of the biogeochemical processing of material exported by the largest rivers of the world takes place in external river plumes located beyond the boundaries of estuarine systems. The estuarine residence time of such large rivers (e.g., Amazon, Ganges, Zaire…) was thus assumed to be negligible (Dürr et al., 2011; Laruelle et al., 2013). The remaining estuarine systems with no τ_k estimate were assigned type-specific median residence times for four different geomorphological classes of estuaries (Laruelle et al., 2013). These median residence times were derived from the compiled database and were equal to 0.08, 0.27, 0.78 and 10.2 years for deltas, tidally dominated estuaries, lagoons and fjords, respectively.

The calculation of N_2O emissions from a given water body required computation of TN_{in}, which accounted for terrestrial inputs and N fixation

delivered to the water body, minus the upstream losses by burial and denitrification. Because N fixation (Fix) depends on the relative availability of P (Equations S6–S7), the computation of N_2O fluxes required the full coupling of the N and P cycles along the river–reservoir–estuary continuum.

Similar to the procedure in Maavara et al. (2017), we obtained the average terrestrial DIN, DON, PN, DIP, DOP and PP yields (Y in mol km^{-2} year^{-1}) from the undammed catchment area upstream of each dam and estuary from NEWS (Mayorga et al., 2010). However, instead of using the average yield per STN-30p basin as in NEWS, we refined the approach to account for the spatial variability in terrestrial N and P sources within each watershed. Based on the input data used in NEWS (Bouwman, Beusen, & Billen, 2009; Van Drecht, Bouwman, Harrison, & Knoop, 2009), we reproduced the spatially explicit representation of N and P sources at a 0.5° resolution. Nutrient loads to the undammed upstream catchment area of a given reservoir or estuary, $F_{k,\text{in,undammed}}$ (mol/year), were then calculated as:

$$F_{k,in,undammed} = W_{k,undammed} \times Y_k \quad (16)$$

where Y_k is the yield for that watershed area (mol km^{-2} year^{-1}) and $W_{k,undammed}$ is the undammed catchment area lying directly upstream of the dam (see Section S2).

N inputs along the aquatic continuum via N fixation were calculated using Equations S6 and S7. Losses via denitrification were computed with Equation (9), while burial in reservoirs was calculated using the following equation fitted to the results of the Monte Carlo simulations:

$$TN_{burial} = (TN_{in} + Fix)[0.51 \times erf(0.4723\,\tau_r)];\ R^2 = 0.50 \quad (17)$$

The global equation derived in Maavara et al. (2015) was used to estimate the corresponding burial fluxes of TP. Reduction of the N load by denitrification and addition via N fixation were calculated for main stem river reaches transporting N downstream from a dam, yielding an “effective” load to the next downstream reservoir or receiving estuary. N burial in river systems, which primarily takes place in adjacent floodplains, occurs via a different mechanism than reservoirs and we therefore did not generate river residence time-dependent retention equations or attempted to estimate this process (Aufdenkampe et al., 2011).

The net nutrient loads delivered to a given dam or estuary can be summarized as:

$$F_{k,in} = \sum_1^n F_{k+1,out,eff} + F_{k,out,undammed} \quad (18)$$

where $F_{k,\text{in}}$ is the flux into the reservoir or estuary k, $\sum_1^n F_{k+1,out,eff}$ is the sum of all effective fluxes discharging from dams upstream of reservoir or estuary k (if any), and $F_{k,out,undammed}$ is the flux from the undammed catchment area, with denitrification and N fixation accounted for. N_2O emissions from

undammed river reaches and main stems downstream of dams were summed to yield the total river emissions reported in Table 2.

TABLE 2 Summary of scenarios used to estimate N_2O emissions, and predicted emissions for rivers, reservoirs and estuaries

Scenario	$EF(b)_{denit}$	$EF(c)_{nitrif}$	Gradient with atmosphere considered?	Rivers	Reservoirs	Estuaries
UQ1	0.3%	0.3%	No	D = 0.57 *N* = 0.61 T = 1.18	D = 0.79 *N* = 0.91 T = 1.70	D = 1.65 *N* = 2.06 T = 3.71
UQ2	3%	3%	No	D = 5.67 *N* = 6.10 T = 11.8	D = 7.89 *N* = 9.14 T = 17.0	D = 16.5 *N* = 20.6 T = 37.1
DS1	0.9%	0.9%	No	D = 1.70 *N* = 1.83 T = 3.53	D = 2.37 *N* = 2.74 T = 5.11	D = 4.95 *N* = 6.18 T = 11.1
DS2	0.9% × 0.4372 erfc (0.4697 τ_r)	0.9%	Yes	D = 1.76 *N* = 1.50 T = 3.26	D = 1.24 *N* = 1.79 T = 3.03	D = 1.31 *N* = 2.97 T = 4.29
UQ3	Burr PDF × 0.4372 erfc (0.4697 τ_r)	Burr PDF	Yes	D = 1.95 *N* = 1.68 T = 3.63	D = 1.38 *N* = 1.82 T = 3.20	D = 1.47 *N* = 3.02 T = 4.48

Note. D: N_2O emissions flux associated with denitrification; N: N_2O emissions flux associated with nitrification; T: total N_2O emissions flux. Units are 10^9 mol/year.

To analyze the global spatial patterns in N_2O emissions, we mapped the combined emissions from rivers, reservoirs and estuaries obtained for DS1 and DS2 at 0.5° resolution. In addition, we plotted the N inputs to the river network and the related N_2O emission factors ($EF(d)$) at the same resolution. A complete description of the method used to perform these calculations can be found in Section S3.

2.5 Scenario-based uncertainty analysis

In addition to the N_2O emission estimates made in DS1 and DS2, we predicted N_2O emissions according to three supplementary scenarios (UQ1–3, Table 2), which helped to contextualize the existing, often contradictory, observations in the literature. UQ1–3 incorporate various EFs and assumptions reported in the literature and, hence, provide insights into the uncertainty associated with the predicted N_2O emissions.

In UQ1 and UQ2, we followed the same assumptions as DS1, but set $EF(b)_{nitrif} = EF(c)_{denit}$ at 3% and 0.3%, respectively, based on Seitzinger and Kroeze (1998). In these scenarios, the transformation of N_2O to N_2 was not explicitly computed; instead, the EFs were assumed to represent net production, that is, all N_2O produced in the water body was assumed to be emitted to the atmosphere. In UQ3, the emission was calculated as in DS2: consumption of N_2O via denitrification was accounted for (Equation 10) and only supersaturated N_2O was emitted to the atmosphere. Rather than fixing $EF(c)_{denit} = 0.9\%$ to scale Equation (10), UQ3 randomly generated $EF(c)_{denit}$ values from a Burr distribution fitted to the Beaulieu et al. (2011) data which range from 0.04% to 5.63%. $EF(c)_{nitrif}$ values were generated from the same Burr distribution, but independently of $EF(c)_{denit}$.

The Monte Carlo analysis was repeated for UQ3, generating an additional set of 6,000 hypothetical observations from which relationships relating N_2O emissions to water residence times and TN loads were extracted. Upscaling was performed using the same method as in DS2, whereby fitting of the results of the Monte Carlo analysis to Equations (13) and (14) yielded $a = 0.002204$, $b = 1.955$, $c = 0.6801$, $d = -1.131$ and $e = 2.945$ ($R^2 = 0.04$ and 0.57).

3 RESULTS

3.1 Nitrogen input to rivers

According to our re-distributed estimates of allochthonous N inputs to the global river network (after Bouwman et al., 2009; Mayorga et al., 2010; Van Drecht et al., 2009), the total loading amounts to 13.2 T mol year^{-1} (184.3 Tg N year^{-1}), of which 4.39 Tmol year^{-1} (61.4 Tg N year^{-1}) are delivered as DIN, 0.85 Tmol/year (11.9 Tg N year^{-1}) as DON, and the remaining 2.19 Tmol/year (30.7 Tg N year^{-1}) as PN. Note that only 16.5% of the TN input (2.18 Tmol/year) is supplied from catchment areas that are intercepted by at least one dam. The global spatial pattern of allochthonous N inputs to rivers (Figure 2) is characterized by high yields across Europe, the eastern half of North America and Southern and Eastern Asia, in particular for DIN as the dominant fraction of TN. Low yields are observed for dryer regions of North Africa, Central Asia and the Western half of North America.

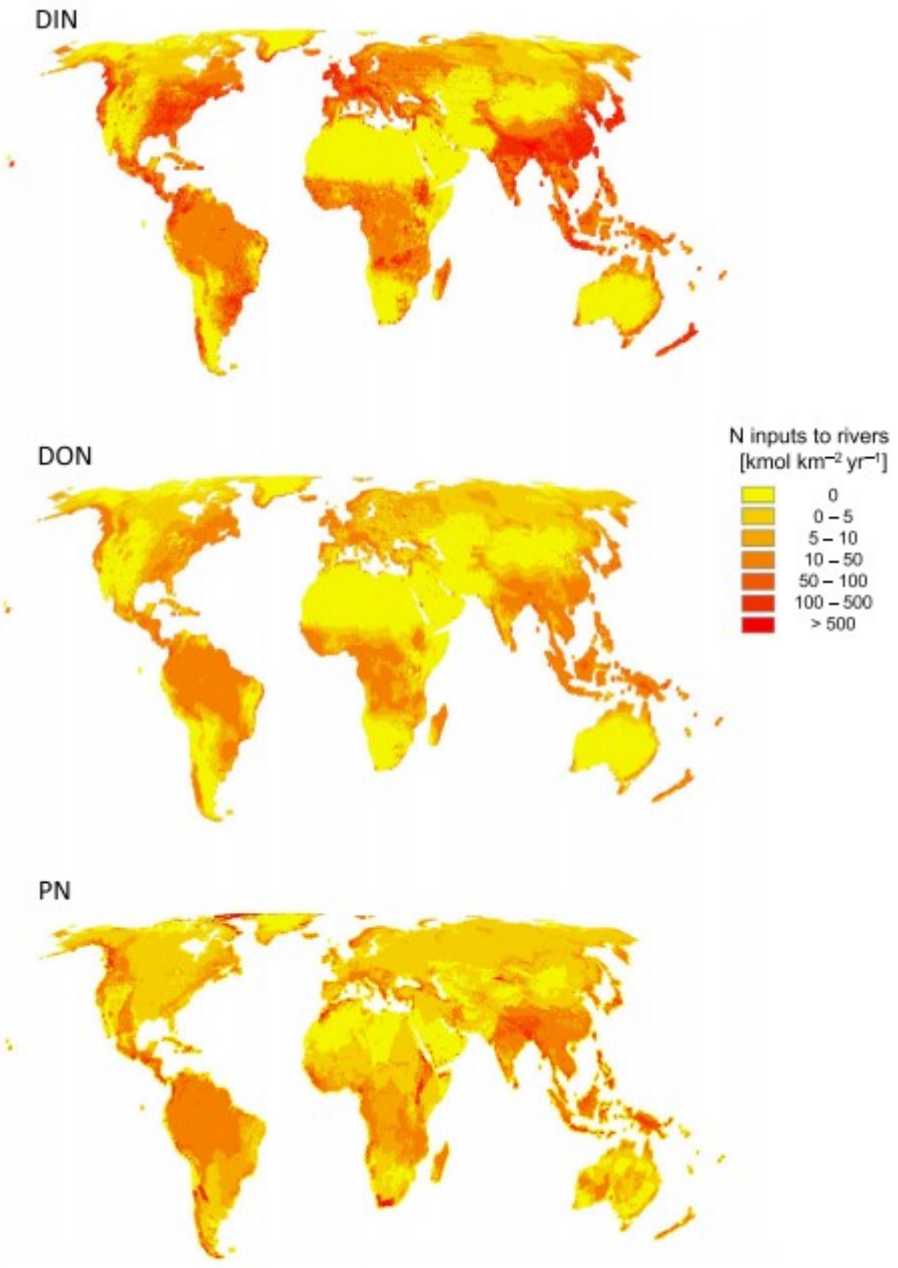

Figure 2. Mobilization of DIN, DON and PN to the river network as prescribed by Global-NEWS, after Van Drecht et al. (2009) and Bouwman et al. (2009), re-distributed at 0.5-degree resolution.

3.2 Nitrification and denitrification fluxes

Worldwide, nitrification fluxes exceed denitrification fluxes in inland waters on average by 5%–20%, depending on the system. Global nitrification fluxes in rivers, reservoirs and estuaries are 0.20 Tmol/year (2.8 Tg N $year^{-1}$), 0.30 Tmol/year (4.3 Tg N $year^{-1}$) and 0.69 Tmol/year (9.6 Tg N $year^{-1}$), respectively. In comparison, denitrification fluxes are 0.19, 0.26 and 0.55 Tmol/year (2.6, 3.7 and 7.7 Tg N $year^{-1}$) for rivers, reservoirs and

estuaries, respectively. Upon averaging each water body or stream segment arithmetically, 0.24% of TN_{in} is nitrified in rivers, 27% in reservoirs, 22% in estuaries, and 0.22% of TN_{in} is denitrified in rivers, 22% in reservoirs and 17% in estuaries. On a per-watershed basis, the Amazon, Ganges, Nile, St. Lawrence and Mississippi River basins account for 18% and 17% of all the denitrification and nitrification in inland waters worldwide, respectively (Figures S3 and S4), with the Amazon accounting for a third of both values. In what follows, we briefly compare our results with global denitrification fluxes published in the literature. A similar comparison is not possible for nitrification, as there are no previous global scale nitrification flux estimates for inland waters.

Our low denitrification estimate in river systems can partly be explained by the exclusion of denitrification occurring in groundwater and riparian zones (Laursen & Seitzinger, 2002; Marzadri, Dee, Tonina, Bellin, & Tank, 2017; Saunders & Kalff, 2001) in our modeling approach. Our results predict that the maximum proportion of TN delivered to river reaches that is lost via denitrification is 18%. In existing studies, watershed-scale denitrification losses have been suggested to be as high as 65% using empirical relationships from regional datasets (McCrackin, Harrison, & Compton, 2014; Seitzinger et al., 2002). However, these studies include the effects of reservoirs in basin-wide budgets, which increases the contribution of denitrification substantially. Indeed, when we account for riverine plus reservoir denitrification, up to 57% of the TN load to river basins is removed via denitrification (with a few exceptions in watersheds with extremely high N fixation), which is in good agreement with the 65% loss cited above. Overall, our results highlight that for most river networks worldwide, N loss via denitrification along undammed river stretches rarely exceeds a few percent, due to their short residence times (median = 1.2 days and mean = 4 days; Figure 5).

Denitrification rates reported for individual reservoirs vary from 0.01 to 108 g N m^{-2} $year^{-1}$ (David, Wall, Royer, & Tank, 2006; Grantz, Kogo, & Scott, 2012; Han, Lu, Burger, Joshi, & Zhang, 2014; Koszelnik, Tomaszek, & Gruca-Rokosz, 2007). Local studies have shown that denitrification usually accounts for between 4% and 58% of the elimination of TN_{in} supplied to reservoirs (David et al., 2006; Garnier, Leporcq, Sanchez, & Philippon, 1999; Koszelnik et al., 2007; Kunz et al., 2011). Globally, only Seitzinger et al. (2006) differentiated between N removal mechanisms in reservoirs, and proposed that denitrification originating from land-derived N in lakes and reservoirs falls in between 19 to 43 Tg N $year^{-1}$, an order of magnitude larger than our estimates.

Published estimates of the denitrification efficiency (in % N loss) in estuaries vary between 10% and 75% of TN_{in} (An & Joye, 2001; Eyre, Ferguson, Webb, Maher, & Oakes, 2011; Eyre, Maher, & Sanders, 2016; Nixon et al., 1996; Seitzinger, 1987; Smyth et al., 2013). However, most systems displaying very high denitrification efficiencies are tropical shallow oligotrophic systems

with extensive sea grass coverage (Eyre et al., 2016; Smyth et al., 2013), which are not representative of the global coastline (Dürr et al., 2011). The bulk of the remaining estimates falls in the 10%–50% range, which is consistent with our results where estuarine systems characterized by short residence times of several days like small deltas only denitrify a few percent of TN_{in}, while systems such as fjords with residence times of several years denitrify up to 38% of TN_{in}. Our results are also in line with the study of Volta, Laruelle, Arndt, and Regnier (2016) who used a generic, physically based estuarine modeling approach spanning a wide range of estuarine geometries; these authors report mean N losses via denitrification in the range 15%–25%.

3.3 Global N_2O emissions from inland waters

Our results indicate that the IPCC EF(*d*) values for rivers and estuaries of 0.25% for denitrification only and 0.75% for denitrification plus nitrification (Mosier et al., 1998), or 0.25% for both processes (Ciais et al., 2013), are likely over-estimated. The arithmetically averaged catchment-scale EF(*d*) values for denitrification plus nitrification are 0.003% for upland tributaries, 0.007%–0.008% for river main stems, 0.17%–0.44% for reservoirs and 0.11%–0.37% for estuaries, with all values comprised between 0% and 1.2% (note: the ranges given are for scenarios DS1 and DS2). When calculated by dividing the global N_2O emission fluxes by the global TN_{in} fluxes, the EF(*d*) values are 0.025%–0.027% for rivers, 0.07%–0.12% for reservoirs and 0.062%–0.16% for estuaries (Table 1). The two sets of EF(*d*) differ because the latter values depend on the TN_{in} fluxes delivered to the water bodies, in addition to the intrinsic N_2O production dynamics of the different types of water bodies. The higher EF(*d*) values for reservoirs and estuaries compared to those for rivers dominate the global spatial patterns in simulated EF(*d*) values (Figure 3). High EF(*d*) values prevail along the coasts and across North America, Europe, Southern and Eastern Asia, southeast Africa and eastern Australia, where dams are numerous.

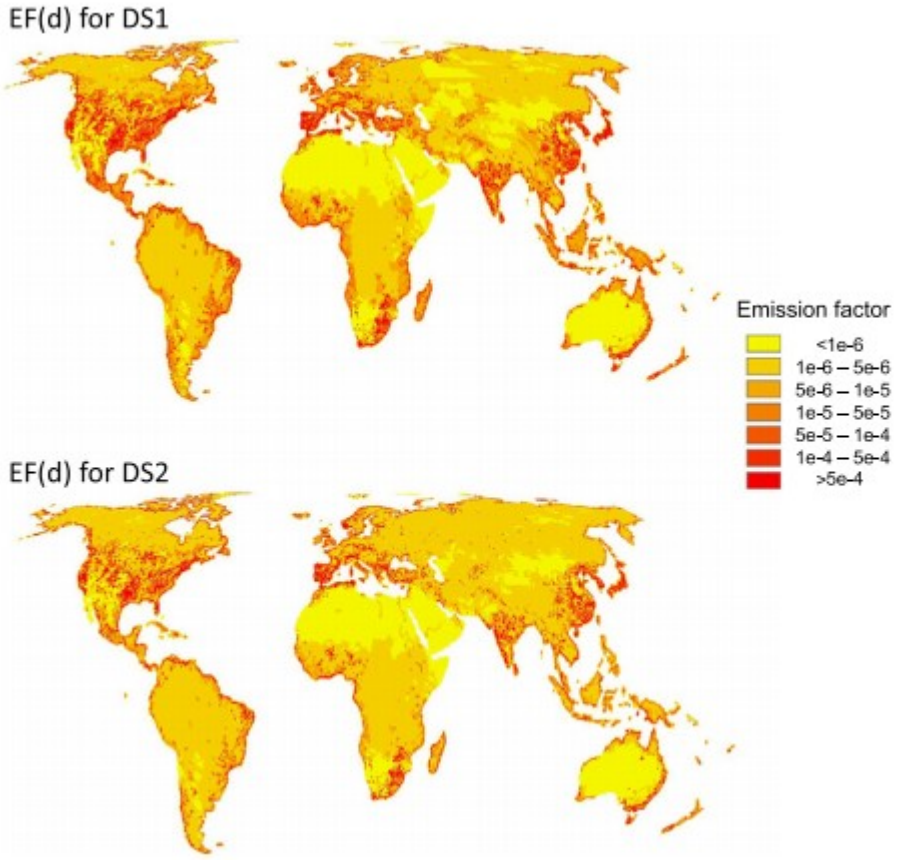

Figure 3. EF(*d*) values per 0.5-degree grid cell for rivers, reservoirs and estuaries worldwide, shown for both default scenarios. The EF(*d*) of rivers is given per 0.5° cell and refers to the residence time within the part of the river network contained in each cell. A river basin consisting of multiple 0.5° cells will have an EF(*d*) that is a weighted average of all grid cell values contained in the basin

We predict worldwide N_2O emissions of 10.6–19.8 Gmol N year^{-1} (148–277 Gg N year^{-1}) for inland waters, 3.03–5.11 Gmol/year (42.4–71.5 Gg N year^{-1}) for reservoirs, 4.29–11.12 Gmol/year (60.0–156 Gg N year^{-1}) for estuaries, and 3.26–3.53 Gmol/year (45.6–49.4 Gg N year^{-1}) for rivers. Generally, spatial patterns in N_2O emission are linked to those of N inputs into river systems (Figure 2), which explains the high emission rates over the populated areas of North America, Europe, Southeast Asia, and throughout the tropics (Figure 4 and Figure S5). The global scale spatial patterns of N_2O emissions are also clearly influenced by the distribution of dams and estuaries. However, other factors can also play a role: Arctic rivers such as the Mackenzie and Yenisei Rivers have basins with small TN yields compared to agricultural watersheds (70th and 33rd percentiles of average yields for all watersheds), but due to the large residence times, they rank in the top 20 watersheds for emissions.

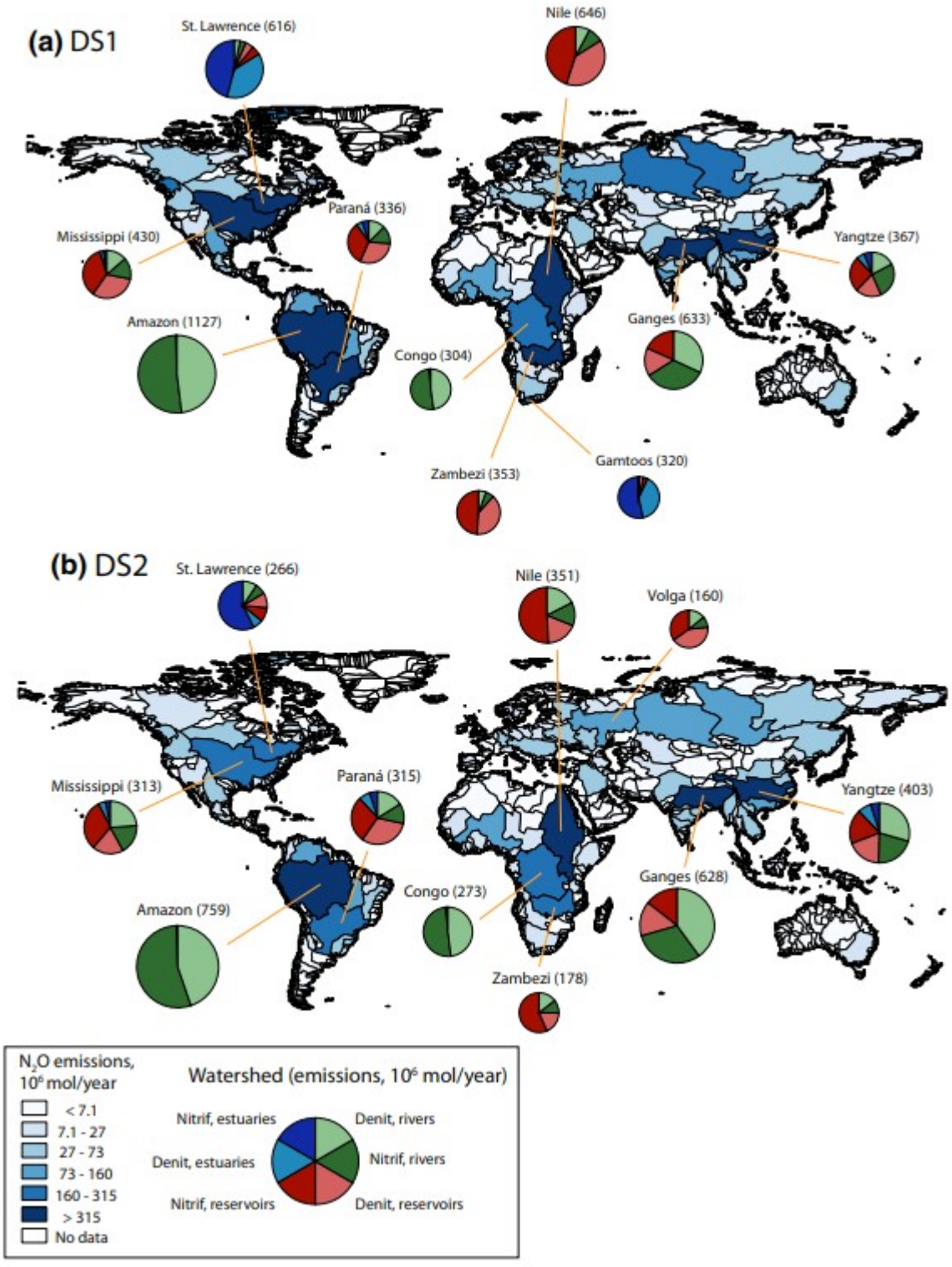

Figure 4. Total N_2O emissions (in 10^6 mol N $year^{-1}$) from rivers, reservoirs and estuaries combined, for major watersheds worldwide in year 2000, for (a) Default scenario 1, and (b) Default scenario 2. Pie charts show the 10 watersheds with the greatest emissions globally, with the size of the chart representing its relative emission flux compared with the other nine watersheds shown (total magnitude of flux shown in brackets after watershed name). The pie charts show the proportion of emissions from denitrification or nitrification in reservoirs, estuaries or rivers.

4 DISCUSSION

4.1 Anthropogenic N_2O emissions

Our estimated inland water N_2O emissions represent 0.8%–1.5% of the 1.28×10^3 Gmol/year of N_2O–N (17.9×10^3 Gg N $year^{-1}$) emitted worldwide (Ciais et al., 2013). Furthermore, our revised NEWS estimates predict that 1.14×10^3 Gmol/year (15.9 Tg N $year^{-1}$) of the total dissolved N (TDN) load to watersheds is anthropogenic in origin, which corresponds to 52% of the TDN load (note: we cannot estimate the proportion of the PN load that is anthropogenic in origin using the NEWS model approach, because enhanced erosion of PN from anthropogenic drivers such as deforestation are not accounted for). We can therefore estimate that 2.6–9.9 Gmol/year additional N_2O-N is evaded from rivers and estuaries due to enhanced anthropogenic loading to watersheds (this range assumes that either all or none of the 14.3 Tg N $year^{-1}$ PN load is anthropogenic in origin), which is at least fivefold lower than Beaulieu et al. (2011) who estimate that 49 Gmol/year (0.68 Tg N $year^{-1}$) of anthropogenic N inputs to river systems are converted to N_2O.

We consider all emissions from reservoirs to be anthropogenic. Reservoirs also alter the riverine fluxes of TN through enhanced denitrification, burial and fixation, affecting the N_2O emission fluxes downstream of dams. Taking into account the effects of dams, we estimate that the total human-driven increase in N_2O emissions from inland waters, relative to pre-industrial conditions, falls in the range 5.6–14.5 Gmol N $year^{-1}$, or 1.1%–3.0% of the 493 Gmol/year (6.9 Tg N $year^{-1}$) anthropogenic N_2O emitted worldwide from all sources combined (Ciais et al., 2013). This flux represents between 23.4 and 60.7 Tg CO_2-equiv. $year^{-1}$. The upper bound of our range is larger than the national emissions from any country in Europe (Janssens-Maenhout et al., 2017). The fact that these are sustained emissions has been shown to be especially problematic from a global warming potential point of view. Neubauer and Megonigal (2015) quantify the global warming potential of sustained emissions, and compared them with pulse fluxes (which is traditionally how global warming potential has been measured). Their results show that even after 500 years, ecosystems must sequester 181 kg of CO_2 to offset 1 kg of N_2O emissions, compared with 132 kg as predicted using the traditional global warming potentials metric.

4.2 System-specific emissions efficiencies and mechanisms

By comparing the results of DS1 and DS2, we can evaluate the effect of explicitly accounting for consumption of N_2O during the last step of denitrification in each water body type (rivers, reservoirs and estuaries). The EF(a) values in Beaulieu et al. (2011) are field measurements and thus may already have been affected to some degree by N_2O consumption. A comparison of the results of DS1 and DS2 therefore provides some measure of the uncertainty associated with using the Beaulieu et al. (2011) data to parameterize N_2O emissions in the model calculations. Essentially, in DS1 we

assume that the field-based EF values account for both N_2O production and consumption during denitrification, while in DS2 they do not include the reduction of N_2O to N_2. Despite the relatively wide ranges predicted in both default scenarios, the relative trends in predicted emissions are quite similar. The estimates for both DS1 and DS2 indicate that estuaries emit more N_2O worldwide than reservoirs or river systems, accounting for 41%–56% of the total emissions fluxes along the LOAC. This reflects their much larger global areal extent (and correspondingly, their volume and residence times) of 1,067 × 10^3 km^2, compared with the smaller 45 × 10^3 km^2 surface area of reservoirs and 662 × 10^3 km^2 of rivers (Table 1).

Per unit area, N_2O emissions from estuaries and rivers are significantly lower than for reservoirs: average surface-area-normalized emission rates are 4.0–10.4 × 10^{-3} mol N m^{-2} $year^{-1}$ for estuaries, 4.9–5.3 × 10^{-3} mol N m^{-2} $year^{-1}$ for rivers, and 67.3–114 × 10^{-3} mol N m^{-2} $year^{-1}$ for reservoirs. The differences in areal emissions largely reflect the residence time distributions of the water bodies (Figure 5). The median residence time for reservoirs is close to 10 months, corresponding to an EF(*d*) of 0.3% in DS1% and 0.2% in DS2. Estuaries, by comparison, have a median residence time of about 3 months, which corresponds to an average EF(*d*) of 0.1% in both scenarios (Figure 5). Water bodies with residence time below 2–3 days, which account for 70% of river systems in our analysis, produce negligible N_2O in both scenarios.

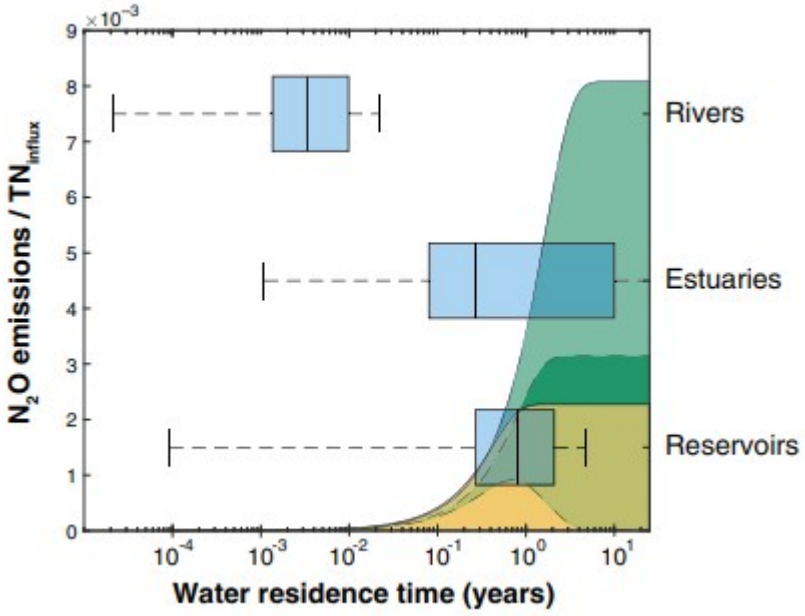

Figure 5. Left axis: N_2O emissions flux, normalized by TN inflow flux to water body, as a function of water residence time. Shaded green curves represent DS1 results where TN_{influx} included riverine and fixation sources, and shaded yellow curves represent DS2 results, where TN_{influx} includes only riverine sources (as per Equations 12-14). In both cases, solid curves show total emissions and dashed curves show the proportion of emissions from denitrification. Box plot (right axis): Distribution of water residence times based on water body type. Solid lines inside boxes are the median, box edges are 1st and 3rd quartiles, whiskers are standard deviations. For clarity, outliers are not shown.

River systems exhibit the lowest emissions of the three systems, directly as a result of their much lower water residence times. When consumption of N_2O via denitrification is explicitly accounted for in DS2, a larger proportion of N_2O emissions originates from denitrification in rivers than in reservoirs and estuaries. At residence times below 6 months, N_2O produced via denitrification exceeds N_2O produced via nitrification (Figure 5). In rivers, 46% of the global N_2O emissions originate from nitrification and 54% from denitrification (Table 2). In DS2, the average $EF(a)_{denit}$ for rivers is 1.2%, compared with the $EF(a)_{nitrif}$ of 0.76%. By comparison, in the same scenario at least 59% of emissions in both reservoirs and estuaries are from nitrification. Hence, in DS2 the N_2O emission flux by denitrification for all rivers worldwide (1.76 Gmol/year) exceeds those for reservoirs (1.24 Gmol/year) and estuaries (1.31 Gmol/year).

The larger role of denitrification as the source of N_2O in river systems is not seen for DS1, where consumption is assumed to have already been accounted for in the EF(a) values reported by Beaulieu et al. (2011). $EF(a)_{nitrif}$ and $EF(a)_{denit}$ are both fixed at 0.9% in this scenario, so any differences between emission pathways are due entirely to the relative magnitudes of the denitrification and nitrification fluxes. Nitrification accounts for a slight majority (52%) of riverine N_2O emissions because of the larger nitrification fluxes predicted at residence times above ~5–6 months (Figure S6). At residence times below 5–6 months, the magnitudes of nitrification and denitrification fluxes are roughly equal (Figure S6), which is why in rivers, which have low residence times, both N_2O production pathways contribute about the same to the global riverine emissions, compared to rivers and estuaries, where nitrification is the dominant pathway (Table 2). A discussion of the mechanisms driving spatially explicit N_2O emissions, and worldwide hotspots, can be found in Section S4.

4.3 Evaluating literature observations

In this section, we first compare our model results with published global-scale N_2O emission estimates for reservoirs and estuaries obtained by scaling up local measurements. We then move on to rivers where previous estimates have all relied on semi-empirical modeling approaches. Additional discussion related to uncertainties in existing literature and field-based studies needed to improve global estimates can be found in Section S5.

4.3.1 Reservoirs and estuaries

Using a bottom-up approach (n = 58), Deemer et al. (2016) obtained a global N_2O emission flux from reservoirs of 2.14 Gmol/year (30 Gg N $year^{-1}$). Despite the entirely different approach, this estimate agrees well with our prediction of 3.03–5.11 Gmol/year. Estimates of N_2O emissions from estuaries vary greatly from 7 to 407 Gmol/year (100 to 5,700 Gg N $year^{-1}$, Table 1). It is worth noting that all estimates higher than 43 Gmol N $year^{-1}$ (600 Gg N $year^{-1}$) were calculated by applying the average emission of a very small number of estuaries (between 1 and 12) to all

estuaries worldwide, possibly implying that the estuaries studied may have disproportionately large emissions relative to the global average. Only the most recent bottom-up estuarine emissions estimate of Murray et al. (2015) and the older estimate of Robinson et al. (1998) overlap with our range of values (Table 1). In contrast, calculations relying on semi-empirical modeling approaches predict emissions on the order of 7 Gmol N $year^{-1}$ (100 Gg N $year^{-1}$) that agree with our range of 4.29–11.1 Gmol N $year^{-1}$ (60.0–156 Gg N $year^{-1}$) (Kroeze et al., 2005, 2010 ; Seitzinger & Kroeze, 1998; Seitzinger et al., 2000).

4.3.2 Rivers

Published estimates of riverine N_2O emissions show the greatest variability of all the water body types considered (Table 1), with the highest values two orders of magnitude larger than the lowest ones (32.2–2,100 Gg N $year^{-1}$). All existing river emission estimates rely on semi-empirical modeling approaches, and thus, the differences are entirely dependent on the predicted loads to rivers, the EF values used and, perhaps most importantly, the assumptions made. For all estimates except one, one of the following sets of assumptions applies:

1. EF(d) = 3% or 0.3%; all of the N load to the river system is nitrified once and half the N load is denitrified once, that is, $EF(a)_{nitrif} = 2\ EF(a)_{denit} = EF(d)$ (as in Kroeze et al., 2005; Seitzinger & Kroeze, 1998; Seitzinger et al., 2000);
2. $EF(a)_{denit} = 0.25\%$ and $EF(a)_{nitrif} = 0.50\%$, with $EF(a)_{denit} + EF(a)_{nitrif} = 0.75\% = EF(d)$ (as in Beaulieu et al., 2011; Mosier et al., 1998), or (ii) $EF(d) = EF(a)_{denit} = EF(a)_{nitrif} = 0.25\%$ (as in Ciais et al., 2013; De Klein et al., 2006; Kroeze et al., 2010). These values also constitute the IPCC guidelines.

Both of these sets of assumptions, however, fail to consider the kinetic limitations imposed by the short water residence times characteristic of most rivers. In our model scenarios, we apply the same EF(a) values as in the above assumptions but introduce a water residence time dependence on EF(d). The corresponding river N_2O emissions fall between 1.18 and 11.8 Gmol N $year^{-1}$ (16.5–165 Gg N $year^{-1}$) (Table 2). These values imply that rivers likely emit significantly less N_2O than proposed in the majority of previous studies, largely because of the limited amount of time available for nitrification and denitrification to occur in most undammed river reaches.

Seitzinger and Kroeze (1998) predict that 75.1 Gmol N $year^{-1}$ of N_2O are emitted from rivers, based on a global DIN load to rivers of 3.0 Tmol/year, assuming that TN:DIN =2:1 and that watersheds yielding more than 10 kg N ha^{-1} $year^{-1}$ have an EF(d) of 3% while the remainder have an EF(d) of 0.3%. In comparison, scenarios UQ1 and UQ2, which bracket the EF(d) range of 3%–0.3%, yield riverine emissions of 1.18–11.8 Gmol/year, with a TN load of 7.42 Tmol/year (104 Tg N $year^{-1}$). Thus, even with a load to rivers

that is less than half that in UQ1 and UQ2, Seitzinger and Kroeze's riverine N_2O emissions far exceed our estimates. We suggest that the assumed denitrification efficiency in Seitzinger and Kroeze (1998), namely that half the N load to rivers is denitrified, is a severe over-estimation and not attainable for the short residence times in these systems. According to our results, on average only 0.22% of TN_{in} is denitrified in undammed river segments while, globally, denitrification in rivers eliminates 1.4% of the total TN_{in} load to watersheds. The large discrepancy is in part explained by the implicit inclusion of higher residence time water bodies such as reservoirs in the older estimates. However, even when we include reservoirs in our calculations only 19% of the global TN loads to river networks is denitrified. Beaulieu et al. (2011) assume that all N_2O produced in rivers is emitted, that is, EF(a) = EF(b) = EF(c) = EF(d) = 0.9%. In DS1 we assume EF(a) = EF(b) = EF(c) = 0.9% but calculate residence time dependent EF(d) values, which yields a mean EF(d) value of 0.004% and a river N_2O emission flux of 3.53 Gmol N $year^{-1}$, much smaller than Beaulieu's 48.6 Gmol N $year^{-1}$ estimate.

To our knowledge, the only study that explicitly departs from either of the two sets of assumptions listed above is that of Hu et al. (2016), who included 6,200 watersheds in their analysis. Our predicted riverine emissions in DS1 and DS2 of 3.26–3.53 Gmol/year (45.6–49.4 Gg N $year^{-1}$), align well with Hu et al.'s prediction of 0.89–4.78 Gmol/year (12.4–66.9 Gg N $year^{-1}$) N_2O emissions. While our calculations were performed at a higher spatial resolution than Hu et al.'s, the general global spatial trends are comparable. In both studies, the largest hotspot for riverine N_2O emissions is Southeast Asia. Furthermore, Hu et al. (2016) predict that 86% of the riverine N_2O outgassing takes place in equatorial and subtropical regions, which is exactly the proportion of global riverine N_2O emissions between 40°N and 40°S according to our simulations. Other regions characterized by high emission rates include western Europe, the Amazonian basin, central Africa and eastern North America. Hu et al. also suggest that commonly used EF estimates are generally too high. They further estimate that EFs relative to DIN loads are somewhere in the range 0.08%–0.31%, based on a statistical analysis in which 82 regression models were tested against a dataset of 169 measured riverine N_2O emissions. Thus, despite using two entirely independent approaches, both our work and that of Hu et al. support the conclusion that previous EFs are overestimated.

4.4 Outlook

Our calculated global N_2O emissions from rivers, reservoirs and estuaries fall in the range 10.6–19.8 Gmol N $year^{-1}$ (148–277 Gg N $year^{-1}$), more than half, and up to an order of magnitude, lower than most studies based on IPCC's guidelines. Despite the much reduced N_2O flux estimates, we find that anthropogenic perturbations to river systems have doubled to quadrupled N_2O emissions from inland waters. We suggest that the IPCC emissions factors of 0.25% and 0.75% are too high to be applied across all rivers,

estuaries and reservoirs. Instead, we estimate the following ranges of emissions factors: 0.004%–0.005% for rivers, 0.17%–0.44% for reservoirs, and 0.11%–0.37% for estuaries. These values, obtained by arithmetically averaging all individual emission factors for a given water body type, directly reflect the water residence time distributions of rivers, reservoirs and estuaries. The majority of emissions in estuaries and reservoirs originate from nitrification, while denitrification tends to dominate in rivers because of the shorter residence times. We find that reservoirs are the most efficient N_2O emitters on a per-area basis, with average areal emissions rates an order of magnitude larger than for rivers and estuaries. We therefore expect worldwide N_2O emissions from inland waters to rise substantially in the coming decades as a result of the ongoing global boom in dam construction (Zarfl, Lumsdon, Berlekamp, Tydecks, & Tockner, 2015), which will nearly double the number of large hydroelectric dams on Earth. A systematic analysis of predicted changes to water residence times caused by these new dams needs to be conducted to aid in forecasting changes in worldwide N_2O emissions.

ACKNOWLEDGEMENTS

This research received funding from the European Union's Horizon 2020 research and innovation programs under the Marie Sklodowska-Curie grant agreement no. 643052 (C-CASCADES project) and under a grant agreement no. 776810 (VERIFY project). TM was funded by a Natural Sciences and Engineering Research Council of Canada (NSERC) postdoctoral fellowship (no. PDF-516575-2018), RL received funding from the European Union's Horizon 2020 research and innovation program under grant agreement no. 703813 for the Marie Sklodowska-Curie European Individual Fellowship “C-Leak,” and GL was supported by Labex L-IPSL, which is funded by ANR (grant #ANR-10-LABX-0018). TM and NJB are supported as part of the Watershed Function Scientific Focus Area funded by the U.S. Department of Energy, Office of Science, Office of Biological and Environmental Research under Award Number DE-AC02-05CH11231.

REFERENCES

Akbarzadeh, Z., Maavara, T., Slowinski, S., & Van Cappellen, P. (in review). Effects of damming on river nitrogen fluxes: A global analysis.

An, S., & Joye, S. B. (2001). Enhancement of coupled nitrification–denitrification by benthic photosynthesis in shallow estuarine sediments. *Limnology and Oceanography*, 46(1), 62– 74. https://doi.org/10.4319/lo.2001.46.1.0062

Aufdenkampe, A. K., Mayorga, E., Raymond, P. A., Melack, J. M., Doney, S. C., Alin, S. R., … Yoo, K. (2011). Riverine coupling of biogeochemical cycles between land, oceans, and atmosphere. *Frontiers in Ecology and the Environment*, 9(1), 53– 60. https://doi.org/10.1890/100014

Bange, H. W. (2006). Nitrous oxide and methane in European coastal waters. *Estuarine, Coastal and Shelf Science*, 70(3), 361– 374. https://doi.org/10.1016/j.ecss.2006.05.042

Bange, H. W., Rapsomanikis, S., & Andreae, M. O. (1996). Nitrous oxide in coastal waters. *Global Biogeochemical Cycles*, 10, 197e207.

Beaulieu, J. J., Tank, J. L., Hamilton, S. K., Wollheim, W. M., Hall, R. O., Mulholland, P. J., … Dahm, C. N. (2011). Nitrous oxide emission from denitrification in stream and river networks. *Proceedings of the National Academy of Sciences of the United States of America*, 108(1), 214– 219. https://doi.org/10.1073/pnas.1011464108

Bouwman, A., Beusen, A. H., & Billen, G. (2009). Human alteration of the global nitrogen and phosphorus soil balances for the period 1970–2050. *Global Biogeochemical Cycles*, 23(4). https://doi.org/10.1029/2009GB003576

Ciais, P., Sabine, C., Bala, G., Bopp, L., Brovkin, V., Canadell, J., …Heimann, M. (2013). Carbon and other biogeochemical cycles. Retrieved from Cambridge, UK and New York, NY.

Clough, T., Buckthought, L., Casciotti, K., Kelliher, F., & Jones, P. (2011). Nitrous oxide dynamics in a braided river system, New Zealand. *Journal of Environmental Quality*, 40(5), 1532– 1541. https://doi.org/10.2134/jeq2010.0527

Clough, T. J., Buckthought, L. E., Kelliher, F. M., & Sherlock, R. R. (2007). Diurnal fluctuations of dissolved nitrous oxide (N_2O) concentrations and estimates of N_2O emissions from a spring-fed river: Implications for IPCC methodology. *Global Change Biology*, 13(5), 1016– 1027.

David, M. B., Wall, L. G., Royer, T. V., & Tank, J. L. (2006). Denitrification and the nitrogen budget of a reservoir in an agricultural landscape. *Ecological Applications*, 16(6), 2177– 2190. https://doi.org/10.1890/1051-0761(2006)016[2177:DATNBO]2.0.CO;2

De Klein, C., Novoa, R. S., Ogle, S., Smith, K. A., Rochette, P., Wirth, T. C., … Walsh, M. (2006). N_2O emissions from managed soils, and CO_2 emissions from lime and urea application. *IPCC Guidelines for National Greenhouse Gas Inventories, Prepared by the National Greenhouse Gas Inventories Programme*, 4, 1– 54.

de Wilde, H. P., & de Bie, M. J. (2000). Nitrous oxide in the Schelde estuary: Production by nitrification and emission to the atmosphere. *Marine Chemistry*, 69(3–4), 203– 216. https://doi.org/10.1016/S0304-4203(99)00106-1

Deemer, B. R., Harrison, J. A., Li, S., Beaulieu, J. J., DelSontro, T., Barros, N., … Vonk, J. A. (2016). Greenhouse gas emissions from reservoir water surfaces: A new global

synthesis. *BioScience*, 66(11), 949– 964. https://doi.org/10.1093/biosci/biw117

Downing, J. A., Cole, J. J., Duarte, C. M., Middelburg, J. J., Melack, J. M., Prairie, Y. T., ... Tranvik, L. J. (2012). Global abundance and size distribution of streams and rivers. *Inland Waters*, 2(4), 229– 236.

Dumont, E., Harrison, J., Kroeze, C., Bakker, E., & Seitzinger, S. (2005). Global distribution and sources of dissolved inorganic nitrogen export to the coastal zone: Results from a spatially explicit, global model. *Global Biogeochemical Cycles*, 19(4). https://doi.org/10.1029/2005GB002488

Dürr, H. H., Laruelle, G. G., van Kempen, C. M., Slomp, C. P., Meybeck, M., & Middelkoop, H. (2011). Worldwide typology of nearshore coastal systems: Defining the estuarine filter of river inputs to the oceans. *Estuaries and Coasts*, 34(3), 441– 458. https://doi.org/10.1007/s12237-011-9381-y

Eyre, B. D., Ferguson, A. J., Webb, A., Maher, D., & Oakes, J. M. (2011). Denitrification, N-fixation and nitrogen and phosphorus fluxes in different benthic habitats and their contribution to the nitrogen and phosphorus budgets of a shallow oligotrophic sub-tropical coastal system (southern Moreton Bay, Australia). *Biogeochemistry*, 102(1–3), 111– 133. https://doi.org/10.1007/s10533-010-9425-6

Eyre, B. D., Maher, D. T., & Sanders, C. (2016). The contribution of denitrification and burial to the nitrogen budgets of three geomorphically distinct Australian estuaries: Importance of seagrass habitats. *Limnology and Oceanography*, 61(3), 1144– 1156. https://doi.org/10.1002/lno.10280

Freing, A., Wallace, D. W., & Bange, H. W. (2012). Global oceanic production of nitrous oxide. *Philosophical Transactions of the Royal Society of London B: Biological Sciences*, 367(1593), 1245– 1255. https://doi.org/10.1098/rstb.2011.0360

Garnier, J., Leporcq, B., Sanchez, N., & Philippon, X. (1999). Biogeochemical mass-balances (C, N, P, Si) in three large reservoirs of the Seine Basin (France). *Biogeochemistry*, 47(2), 119– 146. https://doi.org/10.1007/BF00994919

Grantz, E. M., Kogo, A., & Scott, J. T. (2012). Partitioning whole-lake denitrification using in situ dinitrogen gas accumulation and intact sediment core experiments. *Limnology and Oceanography*, 57(4), 925– 935. https://doi.org/10.4319/lo.2012.57.4.0925

Han, H., Lu, X., Burger, D. F., Joshi, U. M., & Zhang, L. (2014). Nitrogen dynamics at the sediment–water interface in a tropical reservoir. *Ecological Engineering*, 73, 146– 153. https://doi.org/10.1016/j.ecoleng.2014.09.016

Hu, M., Chen, D., & Dahlgren, R. A. (2016). Modeling nitrous oxide emission from rivers: A global assessment. *Global Change Biology*, 22(11), 3566– 3582. https://doi.org/10.1111/gcb.13351

Ivens, W. P., Tysmans, D. J., Kroeze, C., Löhr, A. J., & van Wijnen, J. (2011). Modeling global N_2O emissions from aquatic systems. *Current Opinion in Environmental Sustainability*, 3(5), 350– 358. https://doi.org/10.1016/j.cosust.2011.07.007

Janssens-Maenhout, G., Crippa, M., Guizzardi, D., Muntean, M., Schaaf, E., Olivier, J., ...Schure, K. (2017). Fossil CO_2 and GHG emissions of all world countries (1831–9424). Retrieved from Luxembourg.

Koszelnik, P., Tomaszek, J. A., & Gruca-Rokosz, R. (2007). The significance of denitrification in relation to external loading and nitrogen retention in a mountain reservoir. *Marine and Freshwater Research*, 58(9), 818– 826. https://doi.org/10.1071/MF07012

Kroeze, C., Dumont, E., & Seitzinger, S. P. (2005). New estimates of global emissions of N_2O from rivers and estuaries. *Environmental Sciences*, 2(2– 3), 159– 165.

Kroeze, C., Dumont, E., & Seitzinger, S. (2010). Future trends in emissions of N_2O from rivers and estuaries. *Journal of Integrative Environmental Sciences*, 7(S1), 71– 78.

Kunz, M. J., Anselmetti, F. S., Wüest, A., Wehrli, B., Vollenweider, A., Thüring, S., & Senn, D. B. (2011). Sediment accumulation and carbon, nitrogen, and phosphorus deposition in the large tropical reservoir Lake Kariba (Zambia/Zimbabwe). *Journal of Geophysical Research: Biogeosciences*, 116(G3), https://doi.org/10.1029/2010JG001538

Laruelle, G. G., Durr, H. H., Lauerwald, R., Hartmann, J., Slomp, C. P., Goossens, N., & Regnier, P. A. G. (2013). Global multi-scale segmentation of continental and coastal waters from the watersheds to the continental margins. *Hydrology and Earth System Sciences*, 17(5), 2029– 2051. https://doi.org/10.5194/hess-17-2029-2013

Lauerwald, R., Regnier, P., Camino-Serrano, M., Guenet, B., Guimberteau, M., Ducharne, A., ... Ciais, P. (2017). ORCHILEAK (revision 3875): A new model branch to simulate carbon transfers along the terrestrial–aquatic continuum of the Amazon basin. *Geoscientific Model Development*, 10(10), 3821. https://doi.org/10.5194/gmd-10-3821-2017

Laursen, A. E., & Seitzinger, S. P. (2002). Measurement of denitrification in rivers: An integrated, whole reach approach. *Hydrobiologia*, 485(1– 3), 67– 81.

Law, C., Rees, A., & Owens, N. (1992). Nitrous oxide: Estuarine sources and atmospheric flux. *Estuarine, Coastal and Shelf Science*, 35(3), 301– 314. https://doi.org/10.1016/S0272-7714(05)80050-2

Lehner, B., Liermann, C. R., Revenga, C., Vorosmarty, C., Fekete, B., Crouzet, P., ... Wisser, D. (2011). High-resolution mapping of the world's reservoirs and dams for sustainable river-flow management. *Frontiers in Ecology and the Environment*, 9(9), 494– 502. https://doi.org/10.1890/100125

Lehner, B., Verdin, K., & Jarvis, A. (2008). New global hydrography derived from spaceborne elevation data. *Eos, Transactions American Geophysical Union*, 89(10), 93– 94. https://doi.org/10.1029/2008EO100001

Maavara, T., Lauerwald, R., Regnier, P., & Van Cappellen, P. (2017). Global perturbation of organic carbon cycling by river damming. *Nature Communications*, 8, 15347.

Maavara, T., Parsons, C. T., Ridenour, C., Stojanovic, S., Dürr, H. H., Powley, H. R., & Van Cappellen, P. (2015). Global phosphorus retention by river damming. *Proceedings of the National Academy of Sciences of the United States of America*, 112(51), 15603– 15608. https://doi.org/10.1073/pnas.1511797112

Macdonald, B., Nadelko, A., Chang, Y., Glover, M., & Warneke, S. (2016). Contribution of the cotton irrigation network to farm nitrous oxide emissions. *Soil Research*, 54(5), 651– 658. https://doi.org/10.1071/SR15273

Marzadri, A., Dee, M. M., Tonina, D., Bellin, A., & Tank, J. L. (2017). Role of surface and subsurface processes in scaling N_2O emissions along riverine networks. *Proceedings of the National Academy of Sciences of the United States of America*, 114(17), 4330– 4335.

Mayorga, E., Seitzinger, S. P., Harrison, J. A., Dumont, E., Beusen, A. H. W., Bouwman, A. F., … Van Drecht, G. (2010). Global Nutrient Export from WaterSheds 2 (NEWS 2): Model development and implementation. *Environmental Modelling & Software*, 25(7), 837– 853. https://doi.org/10.1016/j.envsoft.2010.01.007

McCrackin, M. L., Harrison, J. A., & Compton, J. E. (2014). Factors influencing export of dissolved inorganic nitrogen by major rivers: A new, seasonal, spatially explicit, global model. *Global Biogeochemical Cycles*, 28(3), 269– 285. https://doi.org/10.1002/2013GB004723

McKee, B., Aller, R., Allison, M., Bianchi, T., & Kineke, G. (2004). Transport and transformation of dissolved and particulate materials on continental margins influenced by major rivers: Benthic boundary layer and seabed processes. *Continental Shelf Research*, 24(7–8), 899– 926. https://doi.org/10.1016/j.csr.2004.02.009

Mosier, A., Kroeze, C., Nevison, C., Oenema, O., Seitzinger, S., & Van Cleemput, O. (1998). Closing the global N_2O budget: Nitrous oxide emissions through the agricultural nitrogen cycle. *Nutrient Cycling in Agroecosystems*, 52(2–3), 225– 248.

Murray, R. H., Erler, D. V., & Eyre, B. D. (2015). Nitrous oxide fluxes in estuarine environments: Response to global change. *Global Change Biology*, 21(9), 3219– 3245. https://doi.org/10.1111/gcb.12923

Neubauer, S. C., & Megonigal, J. P. (2015). Moving beyond global warming potentials to quantify the climatic role of

ecosystems. *Ecosystems*, 18(6), 1000– 1013. https://doi.org/10.1007/s10021-015-9879-4

Nixon, S., Ammerman, J., Atkinson, L., Berounsky, V., Billen, G., Boicourt, W., … Elmgren, R. (1996). The fate of nitrogen and phosphorus at the land-sea margin of the North Atlantic Ocean. *Biogeochemistry*, 35(1), 141– 180. https://doi.org/10.1007/BF02179826

Ravishankara, A., Daniel, J. S., & Portmann, R. W. (2009). Nitrous oxide (N_2O): The dominant ozone-depleting substance emitted in the 21st century. *Science*, 326(5949), 123– 125.

Robinson, A., Nedwell, D., Harrison, R., & Ogilvie, B. (1998). Hypernutrified estuaries as sources of N_2O emission to the atmosphere: The estuary of the River Colne, Essex, UK. *Marine Ecology Progress Series*, 59– 71. https://doi.org/10.3354/meps164059

Rosso, R., Bacchi, B., & La Barbera, P. (1991). Fractal relation of mainstream length to catchment area in river networks. *Water Resources Research*, 27(3), 381– 387. https://doi.org/10.1029/90WR02404

Saunders, D. L., & Kalff, J. (2001). Nitrogen retention in wetlands, lakes and rivers. *Hydrobiologia*, 443(1), 205– 212. https://doi.org/10.1023/a:1017506914063

Schulze, K., Hunger, M., & Döll, P. (2005). Simulating river flow velocity on global scale. *Advances in Geosciences*, 5, 133– 136. https://doi.org/10.5194/adgeo-5-133-2005

Seitzinger, S. P. (1987). Nitrogen biogeochemistry in an unpolluted estuary: The importance of benthic denitrification. *Marine Ecology Progress Series*, 177– 186. https://doi.org/10.3354/meps041177

Seitzinger, S., Harrison, J. A., Böhlke, J. K., Bouwman, A. F., Lowrance, R., Peterson, B., … Drecht, G. V. (2006). Denitrification across landscapes and waterscapes: A synthesis. *Ecological Applications*, 16(6), 2064– 2090. https://doi.org/10.1890/1051-0761(2006)016[2064:DALAWA]2.0.CO;2

Seitzinger, S. P., Harrison, J., Dumont, E., Beusen, A. H., & Bouwman, A. (2005). Sources and delivery of carbon, nitrogen, and phosphorus to the coastal zone: An overview of Global Nutrient Export from Watersheds (NEWS) models and their application. *Global Biogeochemical Cycles*, 19(4). https://doi.org/10.1029/2005GB002606

Seitzinger, S. P., & Kroeze, C. (1998). Global distribution of nitrous oxide production and N inputs in freshwater and coastal marine ecosystems. *Global Biogeochemical Cycles*, 12(1), 93– 113. https://doi.org/10.1029/97GB03657

Seitzinger, S. P., Kroeze, C., & Styles, R. V. (2000). Global distribution of N_2O emissions from aquatic systems: Natural emissions and anthropogenic effects. *Chemosphere-Global Change Science*, 2(3– 4), 267– 279. https://doi.org/10.1016/S1465-9972(00)00015-5

Seitzinger, S. P., Styles, R. V., Boyer, E. W., Alexander, R. B., Billen, G., Howarth, R. W., … VanBreemen, N. (2002). Nitrogen retention in rivers: Model development and application to watersheds in the northeastern U.S.A. In E. W. Boyer, & R. W. Howarth (Eds.), *The nitrogen cycle at regional to global scales* (pp. 199– 237). Dordrecht, The Netherlands: Springer.

Shen, X., Anagnostou, E. N., Mei, Y., & Hong, Y. (2017). A global distributed basin morphometric dataset. *Scientific Data*, 4, 160124.

Smyth, A. R., Thompson, S. P., Siporin, K. N., Gardner, W. S., McCarthy, M. J., & Piehler, M. F. (2013). Assessing nitrogen dynamics throughout the estuarine landscape. *Estuaries and Coasts*, 36(1), 44– 55. https://doi.org/10.1007/s12237-012-9554-3

Syakila, A., & Kroeze, C. (2011). The global nitrous oxide budget revisited. *Greenhouse Gas Measurement and Management*, 1(1), 17– 26. https://doi.org/10.3763/ghgmm.2010.0007

USGS (2000). HYDRO1k elevation derivative database. Retrieved from https://edcdaac.usgs.gov/gtopo30/hydro/

Van Drecht, G., Bouwman, A., Harrison, J., & Knoop, J. (2009). Global nitrogen and phosphate in urban wastewater for the period 1970 to 2050. *Global Biogeochemical Cycles*, 23(4). https://doi.org/10.1029/2009GB003458

Volta, C., Laruelle, G. G., Arndt, S., & Regnier, P. (2016). Linking biogeochemistry to hydro-geometrical variability in tidal estuaries: A generic modeling approach. *Hydrology and Earth System Sciences*, 20(3), 991– 1030. https://doi.org/10.5194/hess-20-991-2016

Woodwell, G. M., Rich, P. H., & Hall, C. A. S. (1973). Carbon in estuaries. In G. M. Woodwell, & E. V. Pecan (Eds.), *Carbon in the biosphere* (pp. 221– 240). Virginia: Springfield.

Yu, Z., Deng, H., Wang, D., Ye, M., Tan, Y., Li, Y., … Xu, S. (2013). Nitrous oxide emissions in the Shanghai river network: Implications for the effects of urban sewage and IPCC methodology. *Global Change Biology*, 19(10), 2999– 3010. https://doi.org/10.1111/gcb.12290

Zarfl, C., Lumsdon, A. E., Berlekamp, J., Tydecks, L., & Tockner, K. (2015). A global boom in hydropower dam construction. *Aquatic Sciences*, 77(1), 161– 170. https://doi.org/10.1007/s00027-014-0377-0